12^{th} International Conference on Fracture Mechanics of Concrete and Concrete Structures
FraMCoS-12
B.L.A. Pichler, Ch. Hellmich, P. Preinstorfer (Eds)

https://doi.org/10.21012/FC12.1364
MS06-2:1

X-RAY AND NEUTRON IMAGING FOR STEEL CORROSION IN CONCRETE: ADDRESSING CHALLENGES AND REVEALING OPPORTUNITIES

ANDREAS ALHEDE*, JELKE DIJKSTRA† AND KARIN LUNDGREN†

* Chalmers University of Technology, Department of Architecture and Civil Engineering
412 96 Gothenburg, Sweden
e-mail: andreas.alhede@chalmers.se

†Chalmers University of Technology, Department of Architecture and Civil Engineering
412 96 Gothenburg, Sweden

Key words: Reinforced Concrete, Steel Corrosion, X-ray and Neutron Computed Tomography

Abstract: A key challenge in experimental research on steel corrosion in reinforced concrete is the destructive nature of most experimental techniques, which limits the ability to monitor progressive deterioration over time. Advancements in research on steel corrosion in reinforced concrete, however, have been made through the application of non-destructive imaging techniques, particularly X-ray and Neutron Computed Tomography (XCT and NCT). These techniques enable qualitative and quantitative assessments of steel corrosion in concrete.

X-ray attenuation generally increases with the atomic number (density) of the material, making XCT particularly effective for identifying voids in the specimen. In contrast, neutrons interact with the atomic nuclei and are sensitive to light elements, such as hydrogen, making NCT advantageous for identifying moisture and corrosion products in the sample. Effective implementation requires meticulously experimental planning to ensure high-quality data and efficient post-processing.

Sophisticated image analysis methods, such as a multimodal approach that exploits the statistics of both the X-ray and neutron attenuation fields, facilitate phase segmentation of the sample, thereby enabling detailed insights into factors such as the corrosion morphology and the influence of interfacial voids on pitting corrosion. Additionally, time-resolved imaging combined with digital volume correlation enable for monitoring the evolution of steel corrosion and damage within the sample.

This paper aims to provide insights into the effective application of XCT and NCT for investigating steel corrosion in reinforced concrete, focusing on the challenges and opportunities these techniques present for continuous, non-destructive monitoring. Through illustrative examples, this paper demonstrates how these imaging techniques can improve the understanding of steel corrosion in reinforced concrete.

1 INTRODUCTION

Steel corrosion in reinforced concrete is a widespread deterioration mechanism, especially in structures exposed to aggressive chloride-rich environments. Despite substantial research efforts, the complex chemical and physical interactions that drive this electrochemical process are not yet fully understood [1].

One of the primary challenges in advancing the understanding of the corrosion process is the limited access to the steel-concrete in-

terface, as the concrete cover obstructs direct observation and analysis. Although the condition of the steel can be assessed by extracting the reinforcement, this approach yields only a single, static measurement at a specific point in time. Moreover, this destructive approach permanently damages the steel-concrete interface, obstructing studies on the influence of, for example, interfacial voids, moisture content and micro-cracks on corrosion initiation and propagation [2].

Therefore, non-destructive methods are essential for monitoring the *evolution* of processes at the steel-concrete interface to advance the state-of-the-art. These methods should be capable of providing both qualitative data, such as images, enabling visual observations of the interior of the sample, and quantitative data, which are essential for measuring damage and quantifying corrosion characteristics. Furthermore, quantified image data enables the development of prediction models that are physics based.

The use of tomographic techniques, such as X-ray and Neutron Computed Tomography (XCT and NCT), in the study of cementitious materials has grown significantly in recent years [3, 4]. In particular, research on steel corrosion in concrete has advanced markedly, yielding high-quality data on corrosion characteristics and damage. These include, but are not limited to, insights into the expansion coefficient of corrosion products formed inside the sample and corrosion morphology [5], the influence of interfacial voids on pitting corrosion [6], and data of corrosion-induced matrix damage in the three-dimensional field [7].

While the application of XCT and NCT has led to significant advances in understanding steel corrosion in concrete, achieving high-quality data on corrosion characteristics and damage requires careful attention to the experimental setup. The effectiveness of these techniques depends on several factors, including sample preparation, image acquisition and image data processing. Therefore, the aim of this paper is to share practical insights and recommendations for improving data quality, along with illustrative examples that demonstrates the capabilities of XCT and NCT.

2 X-RAY AND NEUTRON COMPUTED TOMOGRAPHY

X-rays and neutrons interact with matter differently, producing attenuation-based two-dimensional radiographic projections that can be reconstructed into three-dimensional scans. The attenuation of X-rays and neutrons in matter is often assumed to follow the Beer-Lambert Law, where the intensity of transmitted X-rays and neutrons decreases exponentially with the linear attenuation coefficient.

X-rays interact primarily with the electron shell of atoms, making the linear attenuation coefficient dependent on the atomic number of the material, which renders XCT, in general, effective for differentiating materials based on density variations [3]. For example, Fig. 1a, acquired using XCT, shows a cross-sectional slice of a reinforced concrete sample, clearly highlighting the steel reinforcement and voids within the matrix. However, the cement paste and sand are poorly differentiated, due to their similar attenuation coefficient.

In contrast, neutrons interact with the atomic nuclei [8], exhibiting higher attenuation for light elements. This makes NCT particularly effective for distinguishing hydrogen-rich materials from those with lower hydrogen content. Fig. 1b shows the same cross-sectional slice as in Fig. 1a, but with data acquired with NCT. As can be seen, the cement paste and sand, having high and low hydrogen content, respectively, is clearly discernable.

It is important to note that neutron imaging induces radioactivity in the sample due to activation of certain elements within the material. The degree of radioactivity depends on the interaction of the free neutrons with the nuclei of specific elements in the concrete. The half-life of the radioactivity can vary significantly based on the chemical composition of the concrete. In some cases, such as the sample shown in Fig 1b, the radioactivity decayed relatively

quickly, with a half-life of just a few days. In other cases, however, the sample may remain radioactive for much longer periods, see for example [5]. Therefore, when considering NCT for concrete applications, it is essential to account for potential radioactivity induced in the sample. This is particularly critical if the sample is to be handled or further analysed post-scanning, e.g. at other large neutron and synchrotron facilities or the home laboratory.

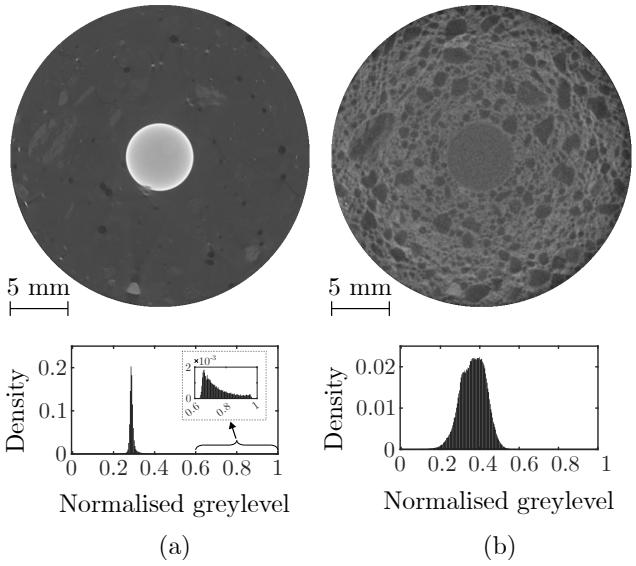

Figure 1: One cross-sectional slice and its distribution of greyscale values for raw data acquired with (a) X-ray computed tomography and (b) Neutron computed tomography

2.1 Image noise

Voxel size and resolution are two distinct concepts, though they are often confused. Voxel size refers to the spatial dimensions of a voxel in the reconstructed image and is influenced by several factors, with the size of the scanned object being one of the most significant. The object size impacts the size of the field of view, as well as the attenuation and scattering of X-ray and neutrons in the sample. Consequently, to obtain a smaller voxel size, the sample geometry must be reduced. However, representing conditions that closely reflect real-world scenarios, such as maintaining an appropriate concrete cover and maximum aggregate size, limits the minimum size of the specimen.

For example, the sample in Fig. 1 was designed with a $10\,\mathrm{mm}$ concrete cover, a maximum sand fraction of $6\,\mathrm{mm}$ and a steel bar with a diameter of $6\,\mathrm{mm}$. This sample geometry resulted in a nominal pixel size of $18.7\,\mu\mathrm{m}$ for XCT and $16.8\,\mu\mathrm{m}$ for NCT.

Resolution refers to the sharpness of the image and is formally measured by the ability to resolve fine details and to distinguish adjacent objects. While voxel size and resolution are closely related, a smaller voxel size does not necessarily translate into an improved resolution, if the contrast mechanism for neutrons (or X-rays) does not allow for this. Smaller voxels amplify noise since fewer X-rays and neutrons are captured per voxel, reducing the signal quality [9]. While extending scan times can partially alleviate this issue, it is less practical for NCT, where scans already require several hours. Furthermore, for sensitive samples, a large radiation dose might damage the sample. Therefore, when designing the sample geometry for imaging analysis, it is essential to consider (1) what physical processes are to be studied and (2) at what scale these processes occur. The resolution needed to accurately capture the processes of interest should guide the design of the sample geometry, ensuring that it is optimised to capture the relevant details without unnecessary amplification of noise.

The high moisture content in concrete, especially in the cement paste, introduces a different type of noise due to the interaction between free neutrons and the hydrogen nuclei in the water. This noise reduces the resolution by masking certain material phases, such as corrosion products, which are also hydrogen-rich.

2.2 Shrinkage

Drying the sample prior to NCT scanning can mitigate moisture-related noise, but this approach introduces another challenge: drying-induced shrinkage in the concrete. For small-scale specimens, this shrinkage can lead to cracking of the concrete [10]. This cracking is particularly problematic in studies investigating corrosion-induced cracking, as it becomes diffi-

cult to separate shrinkage-induced cracks from those caused by corrosion. Furthermore, there is a risk that the initial scan may not capture the sample in its uncracked state, as shrinkage can cause cracking before corrosion occurs. Therefore, it becomes a trade-off between reducing moisture-related noise by drying the sample prior to scanning and minimising the risk of shrinkage-induced cracking.

2.3 Beam hardening

Beam hardening is a common artifact in X-ray imaging, where lower-energy X-rays are absorbed to a higher extent than higher-energy X-rays as the beam penetrates the sample. In a cone-beam geometry, typical of laboratory X-ray sources used in multimodal setups with neutron imaging instruments, these effects are further reinforced by differences in path length. This leads to a beam with higher average (hardened) energy, causing non-linear attenuation [3]. Consequently, the sample appears brighter at its boundaries.

For example, in Fig 1a, the steel reinforcement appears brighter near its boundary compared to its centre, as a result of beam hardening. This artifact not only affects the brightness of the steel but also alters the image contrast at the steel-concrete interface, complicating the segmentation of corrosion products from the surrounding concrete.

To mitigate beam hardening, strategies such as using smaller steel bar diameters or hollow steel bars [10] can be employed to reduce the volume of the steel. Additionally, the effect of non-linear attenuation can be reduced by filtering lower-energy X-rays before the X-ray beam reaches the sample, for example, by placing a copper plate in front of the X-ray source [3].

2.4 Natural and accelerated corrosion

The study of steel corrosion in reinforced concrete can be approached either using specimens subjected to natural or accelerated corrosion, each with distinct advantages and limitations. These two approaches differ in their balance between realism and experimental control, with natural corrosion closely representing real-world conditions and accelerated corrosion enabling controlled, systematic studies of the corrosion process over shorter time periods.

Natural corrosion, on the one hand, can be studied either by coring specimens from existing structures which suffer from corrosion damages, or by designing samples to corrode under realistic environmental conditions in laboratory over longer time periods. The primary advantage of natural corrosion studies is that they represent more realistic conditions, thus providing insights into the corrosion process as it occurs naturally. However, these methods are limited in scope. For example, samples taken from engineering structures only offer a snapshot of the corrosion process at a single time frame, with no imaging data available from previous stages, such as the uncorroded state. This limits the research study to static measures, leaving out studies on the *evolution* of steel corrosion and damage within the specimen.

Accelerated corrosion, on the other hand, involves the careful design of specimens in controlled laboratory environments, where corrosion can be induced at an accelerated rate by applying electrical current. This approach offers advantages such as the ability to monitor the corrosion process in a shorter time frame. Within this period, samples could be scanned repeatedly throughout the corrosion process, allowing for a systematic study on the *evolution* of steel corrosion. However, the accelerated nature of such corrosion tests introduces limitations. The high current densities imposed on the specimens are far greater than those encountered in natural environments [11], potentially altering the corrosion morphology and chemical composition of corrosion products. Consequently, the results may not fully reflect the natural behaviour of steel corrosion in concrete.

3 CORROSION CHARACTERISTICS

Multimodal registration accounts for the differing modalities of XCT and NCT [12], enabling the extraction of complementary information of the sample, which otherwise would

not have been possible. This approach enables a detailed characterisation of various material phases, including steel, sand, cement paste, air voids and corrosion products. An example of such segmentation is presented in Fig. 2, illustrating the material phases at two instances in time: before and after corrosion.

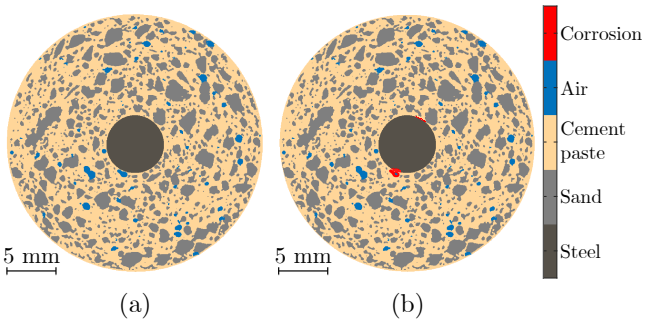

Figure 2: One phase segmented cross-sectional slice of a reinforced mortar sample: (a) before corrosion (b) after corrosion.

The multimodal approach has previously been employed for quantifying the corrosion morphology [5, 7], as well as in more detailed studies that are difficult to conduct without imaging. For example, Angst et al. [6] investigated the influence of interfacial voids on pitting corrosion in cylindrical specimens cored from an engineering structure. They found that pitting corrosion was observed in or in the vicinity of some interfacial voids, but in the majority of the voids, no corrosion attacks were observed. Contrary to this finding, a yet unpublished study by the authors [15] under accelerated corrosion conditions found that when voids were present at the steel-concrete interface, the risk of corrosion increased with the size of the void. Multimodal imaging holds promise for continued studies on this phenomenon, enabling more detailed insights into whether a relationship between interfacial voids and corrosion exists.

The volumetric expansion coefficient of corrosion products, which is two to six times larger that the volume of the virgin steel [1], is a key parameter in modelling of the corrosion and cracking process. However, quantifying this coefficient using destructive techniques is challenging, as corrosion products can react with oxygen when exposed to environmental conditions that differ from those within the cementitious matrix [13]. Imaging techniques provide a non-destructive alternative, allowing for more accurate quantification of the type of oxides formed within the sample.

By analysing interfacial voids partially filled with corrosion products, and assuming that corrosion products within these voids expanded under stress-free conditions, the volumetric expansion coefficient can be determined by dividing the volume of corrosion products with the volume loss of the steel. A previous study reported values of 4.24 and 4.13 for natural corrosion [5]. For accelerated corrosion, slightly lower values have been found: 3.91 [5] and 3.90 [14]. Additionally, yet unpublished work by the authors [15] has found the volumetric expansion coefficient to be very close to those reported for accelerated corrosion (3.90), further highlighting the consistency across independent studies.

Alhede et al. [7] derived an expression for the volumetric strain in the corrosion layer. By performing a phase segmentation of the sample, the volumetric strain can be estimated as

$$\varepsilon_v = \frac{V_{cc}}{\eta \Delta V_s - V_{ca}} - 1 \qquad (1)$$

where V_{cc} and V_{ca} represent the volumes of compressed and uncompressed corrosion products in the sample, respectively. The differentiation of compressed and uncompressed corrosion products was based on the assumption that corrosion products accumulating in partially filled interfacial voids remained uncompressed. Thus, the volume of compressed corrosion products was estimated by subtracting the volume of uncompressed corrosion from the total volume of corrosion products. Additionally, η denotes the volumetric expansion coefficient of corrosion products and ΔV_s is the volume loss of steel. It was shown how the volumetric strain in the corrosion layer becomes increasingly negative as the volumetric expansion coefficient, η, increases.

4 CORROSION-INDUCED DEFORMATIONS IN THE CONCRETE

Experimental data are essential for calibrating and validating phenomenological corrosion models. Traditional methodologies often rely on measuring parameters such as the corrosion penetration at the time of cracking, or the relationship between surface crack width and corrosion level. However, this relationship exhibits significant scatter [16, 17], limiting the reliability for accurately calibrating corrosion models. The variability in results can be attributed to several factors, including different corrosion morphologies across tests, sample geometry, variations in concrete quality, and localized weaknesses in the matrix, all of which contribute to inconsistent measurements.

Traditional approaches primarily provide data from the surface of the specimen, such as surface crack widths. Measurements at the surface, however, are insufficient for capturing the full extent of corrosion-induced damage. In particular, surface measurements cannot accurately reflect internal damage, especially in the early stages of corrosion, when no surface cracks have formed. To obtain data on internal factors, such as corrosion penetration depth and corrosion morphology, destructive methods are often employed. These typically involve extracting the reinforcement bars from the specimen, which yields only static data at a single point in time. Consequently, these methods hinder the ability to continuously monitor the evolving corrosion process over time.

In contrast, XCT and NCT allow for the acquisition of three-dimensional datasets over time, allowing for detailed insights into internal processes. These datasets can be analysed using Digital Volume Correlation (DVC) [18] to measure internal deformations within the sample in three-dimensional space. Previous work has successfully applied this technique to measure corrosion-induced deformations within concrete [7, 19]. Additionally, when datasets are collected at multiple stages of the corrosion process, the time-resolved evolution of internal damage can be monitored.

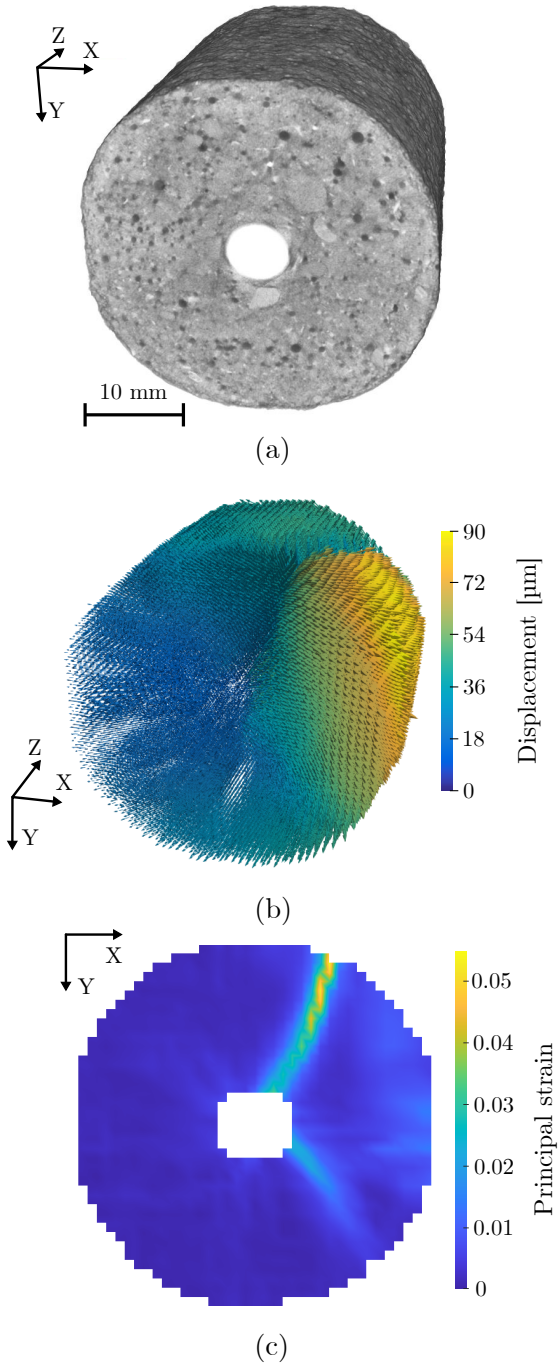

Figure 3: Figure adapted from [19]. Corrosion-induced deformations in the concrete cover (a) rendering of XCT (b) displacement field (c) cross-sectional slice and the distribution of first principal strain.

An example of a DVC analysis is shown in Fig. 3, where corrosion-induced deformations within the concrete cover were measured. Fig. 3a presents a rendering of XCT data of the specimen, which has been exposed to accelerated

corrosion. Two longitudinal cracks are visible in the specimen, although the quality of the rendering was too low to clearly detail these cracks.

In Fig. 3b, the displacement field due to corrosion formation at the steel-concrete interface is shown. This displacement field was measured using XCT data from the initial (uncorroded) configuration of the sample, and subsequent XCT data after corrosion exposure. Upon closer inspection, one can observe displacement vectors pointing in opposite directions in certain regions, indicating localised deformations in the concrete matrix.

Lastly, 3c shows a cross-sectional slice taken from the middle of the sample, illustrating the distribution of first principal strain. In this cross-section, strain localisation can be seen in two regions. These regions corresponds to the locations where concrete cracks have formed within the concrete matrix. This imaging-based approach provides a comprehensive basis for model validation and calibration, complementing traditional methodologies by enabling the measurement of internal corrosion damage.

5 CONCLUSIONS

This paper briefly revealed challenges and opportunities of applying X-ray and neutron computed tomography for studies of steel corrosion in reinforced concrete. Some of the key challenges identified include:

- **Sample size:** The sample size is constrained by the configuration of the scanning equipment, limiting studies to small-scale specimens, typically a few centimetres in diameter.

- **Image noise:** Smaller voxel sizes tend to increase image noise, which can degrade the resolution of the imaging data, masking finer details of interest. Longer scan times only partly alleviate this.

- **Moisture content:** High moisture content within the cementitious matrix increases neutron attenuation, leading to another source of image noise. While prior drying of the sample could reduce this problem, it carries the risk of shrinkage-induced cracking.

- **Beam hardening:** The absorption of lower-energy X-rays more than higher-energy X-rays causes the sample, particularly the steel, to appear brighter near its boundaries. This artifact complicates segmentation of corrosion products at the steel-concrete interface. Filtering of lower-energy X-rays before they reach the sample can reduce this artifact.

- **Natural versus accelerated corrosion:** When investigating cored samples from engineering structures, imaging data can only be obtained at a single point in time, preventing access to imaging data of the uncorroded configuration of the sample. However, natural corrosion can be mimicked by designing samples to corrode under realistic environmental conditions, which allows for multiple scans of the sample over time. In contrast, accelerated corrosion allows repeated scanning throughout the corrosion period, but over a shorter time frame. However, the high current densities used in these tests may alter the corrosion process, potentially masking the results less representative of natural corrosion.

Some of the opportunities with X-ray and neutron computed tomography in the study of steel corrosion can be realised by addressing the challenges outlined above. These include:

- **Corrosion characteristics:** Multimodal X-ray and neutron computed tomography enables detailed phase segmentation of the sample, facilitating quantification of corrosion morphology, the volumetric expansion coefficient of corrosion products, the volumetric strain in the corrosion layer and the study of the influence of interfacial voids on the risk of pitting corrosion.

- **Kinematics:** By acquiring imaging data at various stages in the corrosion process, corrosion-induced deformations within the concrete cover can be measured in the three-dimensional field, providing valuable experimental data on kinematics which can be used for model validation and calibration.

REFERENCES

[1] Tuutti, K. 1982. Corrosion of steel in concrete. *Swedish Cement and Concrete Research Institute.* Stockholm.

[2] Angst, U. A. et al. 2019. The effect of the steel-concrete interface on chloride-induced corrosion initiation in concrete: a critical review by RILEM TC 262-SCI. *Materials and Structures.* **52**:88. doi:10.1617/s11527-019-1387-0.

[3] Brisard, S. and Serdar, M. and Monteiro P. 2020. Multiscale X-ray tomography of cementitious materials: A review. *Cement and Concrete Research.* **128**:105824. doi:10.1016/j.cemconres.2019.105824.

[4] Zhang, P. and Wittmann, F.H. and Lura, P. and Müller, H.S. and Han, S. and Zhao, T. 2018. Application of neutron imaging to investigate fundamental aspects of durability of cement-based materials: A review. *Cement and Concrete Research.* **108**:152-166. doi:10.1016/j.cemconres.2018.03.003.

[5] Robuschi, S. and Tengattini, A. and Dijkstra, J. and Fernandez, I. and Lundgren, K. 2021. A closer look at corrosion of steel reinforcement bars in concrete using 3D neutron and X-ray computed tomography. *Cement and Concrete Research.* **144**:106439. doi:10.1016/j.cemconres.2021.106439.

[6] Angst, U.M. and Rossi, E. and Käthler, C.B. and Mannes, D. and Trtik, P. and Elsener, B. and Zhou, Z. and Strobl, M. 2024. Chloride-induced corrosion of steel in concrete - insights from bimodal neutron and X-ray microtomography combined with ex-situ microscopy. *Materials and Structures.* **57**:56. doi:10.1617/s11527-024-02337-7.

[7] Alhede, A. and Dijkstra, J. and Robuschi, S. and Tengattini, A. and Lundgren, K. 2023. A two-stage study of steel corrosion and internal cracking revealed by multimodal tomography. *Construction and Building Materials.* **394**:132187. doi:10.1016/j.conbuildmat.2023.132187.

[8] Tengattini, A. and Lenoir, N. and Andó, E. and Viggiani, G. 2021. Neutron imaging for geomechanics: A review. *Geomechanics for Energy and the Environment.* **27**:100206. doi:10.1016/j.gete.2020.100206.

[9] Tanimoto, H. and Arai, Y. 2009. The effect of voxel size on image reconstrution in cone-beam computed tomography. *Oral Radiology.* **25**:149-153. doi:10.1007/s11282-009-0019-8.

[10] Alhede, A. and Dijkstra, J. and Lundgren, K. 2023. Monitoring corrosion-induced concrete cracking adjacent to the steel-concrete interface. *Materials and Structures.* **56**:162. doi:10.1617/s11527-023-02252-3.

[11] Alonso, C. and Andrade, C. and Rodriguez, J. and Diez, J.M. 1998. Factors controlling cracking of concrete affected by reinforcement corrosion. *Materials and Structures.* **31**:435-441. doi:10.1007/bf02480466.

[12] Roubin, E. and Andò, E. and Roux, S. 2019. The colours of concrete as seen by X-rays and neutrons. *Cement and Concrete Composites.* **104**:103336. doi:10.1016/j.cemconcomp.2019.103336.

[13] Andrade, C. and Tavares, F. and Toro, L. and Fullea, J. 2011. Observations on the morphology of oxide formation due to reinforcement corrosion. *Modelling of Corroding Concrete Structures.* **5**:179-193. doi:10.1007/978-94-007-0677-4_12.

[14] Sun, H. and Jiang, C. and Cao, K. and Yu, D. and Liu, W. and Zhang, X. and Xing, D. and Zhao, F. 2021. Monitoring of steel corrosion and cracking in cement paste exposed to combined sulfate-chloride attack with X-ray microtomography. *Construction and Building Materials.* **302**:124345. doi:10.1016/j.conbuildmat.2021.124345.

[15] Alhede, A. and Dijkstra, J. and Tengattini, A. and Lundgren, K. 2024. Characterisation of steel corrosion and matrix damage in reinforced mortar combining analytical, electrical and image-based techniques. *Submitted for publication.*

[16] Andrade, C. and Cesetti, A. and Mancini, G. and Tondolo, F. 2016. Estimating corrosion attack in reinforced concrete by means of crack opening. *Structural Concrete.* **17**:4. doi:10.1002/suco.201500114.

[17] Tahershamsi, M. and Fernandez, I. and Lundgren, K. and Zandi, K. 2017. Investigating correlations between crack width, corrosion level and anchorage capacity. *Structure and Infrastructure Engineering.* **13**:10. doi:10.1080/15732479.2016.1263673.

[18] Stamati, O. et al. 2020. spam: Software for Practical Analysis of Materials. *Journal of Open Source Software.* **5**:51. doi:10.21105/joss.02286.

[19] Alhede, A. and Van Steen, C. 2024. Measuring corrosion-induced deformations in reinforced concrete: An image-based approach by means of X-ray computed tomography. In *Lecture Notes in Civil Engineering.* Springer. (in press).